THERMAL EFFECTS ON RAYLEIGH-MARANGONI INSTABILITY IN A LAYER OF NANOFLUID

[1]A. A. ABDULLAH, [2]K. A. LINDSAY, [3]S. A. ALTHOBAITI

[1,2,3]Department of Mathematical Sciences, Faculty of Applied Science, Umm Al-Qura University
E-mail: aamohammad@uqu.edu.sa, Kenneth.lindsay@glasgow.ac.uk, sat21c@hotmail.com

Abstract- These instructions give you guidelines for A linear stability analysis for the onset of Rayleigh-Marangoni convection in a horizontal layer of a nanofluid heated from below is investigated. The model employed for the nanofluid incorporates the effects of Brownian motion and thermophoresis. The lower boundary of the layer is assumed to be a rigid surface at fixed temperature while the top boundary is assumed to be a non-deformable free surface cooled by convection to an exterior region at a fixed temperature. The boundaries of the layer are assumed to be impenetrable to nanoparticles with their distribution being determined from a conservation condition. The linear analysis uses spectral methods based on the expansion of eigenfunctions as Chebyshev series. Stability boundaries for temperature and nanofraction Marangoni numbers and Rayleigh number are obtained for several nanofluids.

Index Terms- Brownian motion, nanofluid, Rayleigh Marangoni stability, thermophoresis.

I. INTRODUCTION

Over the past decade, a new class of fluid called a "nanofluid" have been reported to possess substantially higher thermal conductivity than anticipated from the effective medium theories. A nanofluid refers to a base fluid that contains particles of maximum size 100 nm. Common heat transfer fluids used as base fluids include water and various organic fluids such as kerosene, ethylene glycol and ethanol, while the nanoparticles used include metallic or metallic oxide particles such as copper, copper oxide, alumina (Al$_2$O$_3$) and also multi-walled carbon nanotubules (MWCNTs).

The flow of nanofluid is of great interest in numerous areas of modern science, engineering and technology, the chemical and nuclear industries and bio-mechanics. Nanofluids are not naturally occurring but are synthesized in laboratories. The choice of base fluid and particle combination depends on the application for which the nanofluid is intended. Such fluids are used in industry as coolants, lubricants, for the delivery of drugs, in heat exchangers and in micro-channel heat sinks among other applications (Buongiorno and Hu [1], Tsai and Chein [2], Kleinstreuer et al. [3]).

Buongiorno [4] conducted an extensive study of nanofluids and derived the conservation equations of a non-homogeneous equilibrium model of a nanofluid. This model incorporated the effects of Brownian diffusion and thermophoresis. On the basis of this model, studies were conducted by many authors. Tzou [5], [6] studied the thermal instability of nanofluids (Rayleigh-Benard convection) and showed that nanofluids are less stable than regular fluids. Nield and Kuzentsov [7], [8] and Kuznetsov and Nield [9], [10] studied the onset of convection in a horizontal layer of a porous medium saturated by a nanofluid. Yadav et al. [11] considered the linear stability of Rayleigh-Benard convection in nanofluids with and without rotation, and obtained a sufficient condition for the existence of overstability. Ramesh and Rana [12] considered the effect of rotation on a horizontal layer of porous medium saturated by a nanofluid. The effect of magnetic field on the thermal instability of nanofluids has been discussed by Gupta et al. [13], Yadav et al. [14] and Mahajan and Arora [15]. These authors showed that the presence of a magnetic field has a stabilizing influence. The linear stability of Marangoni convection in a layer of nanofluid has been investigated by Abdullah and Lindsay "to be published" [16]. They showed numerically that for nanofluids, Marangoni instability ensues through overstable convection.

The general trend for base fluids is that their surface tension decreases with increasing temperature. For nanofluids, however, surface tension depends on both temperature and nanoparticle concentration. Experimental studies for different nanofluids have reported that the presence of nanoparticles causes surface tension to be increased, unchanged or decreased.

The earliest work on Rayleigh-Marangoni instability in a fluid layer heated from below was performed by Nield [17] who showed that, buoyancy and surface tension reinforce each other and are tightly coupled. The work of Nield [17] has been extended and polished by many workers for deformable and non-deformable surfaces (e.g. Sarma [18], Garcia-Ybarra et al. [19], Benguria and Depassier [20], Perez-Garcia and Carneiro [21], Hennenberg et al. [22], Hashim and Arfin [23], Zhao et al. [24]).

A survey of the literature revealed that no research has been conducting with regard to the stability of Rayleigh-Marangoni convection in nanofluids. Therefore the object of the present study is to investigate this problem for several types of nanofluid.

II. PROBLEM FORMULATION

Consider an infinite horizontal layer of an incompressible nanofluid confined between the planes

$x_3^* = 0$ and $x_3^* = d$ of a rectangular Cartesian system of coordinates with position vector $x_i^* = x_1^* \underline{e}_1 + x_2^* \underline{e}_2 + x_3^* \underline{e}_3$ with $\underline{e}_3$ directed vertically upwards. Let $T^*(t^*, x_i^*)$ and $\varphi^*(t^*, x_i^*)$ denote respectively the Kelvin temperature and volume fraction of nanoparticles in the fluid at time t^* and position x_i^*. On $x_3^* = 0$ the nanofluid is assumed to rest on a rigid boundary which is maintained at a constant Kelvin temperature T_0, whereas on $x_3^* = d$ the motion of the nanofluid is driven by the thermocapillary effect of the surface tension of the nanofluid, say $\gamma(T^*, \varphi^*)$, but otherwise the surface is non-deformable and loses heat by convection to an environment at constant temperature T_1.

Following Nield and Kuznetsov [8] it is assumed that any changes in temperature and nanoparticle volume fraction taking place across the layer are sufficiently small that the density, viscosity, thermal conductivity and specific heat of the nanofluid may be assumed to behave as constants determined by the nanoparticle volume fraction and the temperature of the layer.

A. Field Equations

Following the work of Buongiorno [4], Tzou [5], [6] and Nield and Kuznetsov [7], the governing equations for a nanofluid in the absence of chemical reactions, but in the presence of thermophoresis are

$$\frac{\partial V_j^*}{\partial x_j^*} = 0, \tag{1}$$

$$\rho(\varphi^*)\left(\frac{\partial V_j^*}{\partial t^*} + V_k^* \frac{\partial V_j^*}{\partial x_k^*}\right) = -\frac{\partial P^*}{\partial x_j^*} + \mu(\varphi^*)\frac{\partial^2 V_j^*}{\partial x_k^* \partial x_k^*} - \rho(\varphi^*) g \delta_{j3}, \tag{2}$$

$$\frac{\partial \varphi^*}{\partial t^*} + V_k^* \frac{\partial \varphi^*}{\partial x_k^*} = -\frac{1}{\rho_p}\frac{\partial J_k^*}{\partial x_k^*}, \tag{3}$$

$$(\rho C)(\varphi^*)\left(\frac{\partial T^*}{\partial t^*} + V_k^* \frac{\partial T^*}{\partial x_k^*}\right) = -\frac{\partial q_k^*}{\partial x_k^*} + h_p(T^*)\frac{\partial J_k^*}{\partial x_k^*}, \tag{4}$$

where V_j^* denotes the nanofluid velocity, g denotes acceleration due to gravity and P^* denotes hydrostatic pressure. The nanofluid density, ρ, dynamic viscosity, μ, and specific heat at constant pressure, C, are defined in terms of the nanoparticle volume fraction, φ^*, by the formulae

$$\rho(\varphi^*) = \varphi^* \rho_p + (1-\varphi^*)\rho_f, \tag{5}$$

$$\mu(\varphi^*) = \mu_f (1-\varphi^*)^{-5/2}, \tag{6}$$

$$(\rho C)(\varphi^*) = \varphi^* \rho_p C_p + (1-\varphi^*)\rho_f C_f. \tag{7}$$

In expression (5) the parameters ρ_f and ρ_p denote respectively the densities of the base fluid and nanoparticle material. Expression (6) is Brinkman's model [25] for dynamic viscosity, where μ_f denotes the dynamic viscosity of the base fluid. Finally, C_f and C_p in expression (7) denote respectively the specific heats of the base fluid and the nanoparticle material. The density of the nanofluid can be approximated by that of the base fluid as adopted by Tzou [5], [6] when φ^* is small. Thus using the Boussinesq approximation the momentum equation (2) becomes

$$\rho_0\left(\frac{\partial V_j^*}{\partial t^*} + V_k^* \frac{\partial V_j^*}{\partial x_k^*}\right) = -\frac{\partial P^*}{\partial x_j^*} + \mu(\varphi^*)\frac{\partial^2 V_j^*}{\partial x_k^* \partial x_k^*} - \left[\varphi^* \rho_p + \rho_0 (1-\varphi^*)\left(1-\beta(T^*-T_0)\right)\right] g \delta_{j3}, \tag{8}$$

where ρ_0 is the nanofluid density at T_0, the Kelvin temperature of the base of the nanoparticle layer. The vector J_k^* in equations (3) and (4) denotes the diffusive mass flux of nanoparticles and is the sum of contributions from Brownian and thermophoresis diffusions, namely

$$J_j^* = -\rho_p\left(D_B \frac{\partial \varphi^*}{\partial x_j^*} + \frac{D_T}{T_0}\frac{\partial T^*}{\partial x_j^*}\right), \tag{9}$$

where D_B and D_T (assumed constants) represent respectively the Brownian and thermophoretic diffusion coefficients with respective constitutive specifications

$$D_B = \frac{K T_0}{3\pi\mu_f d_p}, \qquad D_T = \frac{\mu_f}{\rho_f}\left(\frac{0.26\kappa_f}{2\kappa_f + \kappa_p}\right)\varphi^*. \tag{10}$$

In these expressions k is Boltzman's constant, d_p is the nanoparticle diameter, and κ_f and κ_p are respectively the thermal conductivities of the base fluid and the nanoparticle material. Finally, q_j^* in equation (4) denotes heat flux and has constitutive expression

$$q_j^* = -\kappa(\varphi^*)\frac{\partial T^*}{\partial x_j^*} + h_p(T^*) J_j^*, \tag{11}$$

where $\kappa(\varphi^*)$ denotes the thermal conductivity of the nanofluid and $h_p(T^*)$ denotes the specific enthalpy of the nanoparticle material. Subsequent analyses will assume the Hamilton-Crosser [26] specification of $\kappa(\varphi)$, namely the constitutive equation

$$\frac{\kappa(\varphi)}{\kappa_f} = \frac{(n-1)(1-\varphi)\kappa_f + (n\varphi + 1 - \varphi)\kappa_s}{\kappa_s(1-\varphi) + (n-1+\varphi)\kappa_f}, \tag{12}$$

in which $n = 3/\psi$ denotes the "shape factor" of the nanoparticles and ψ denotes particle sphericity. Typical values of n satisfy 3 < n < 6 (see e.g. Timofeeva et al. [27]) with values near $n = 3$ being associated with nanoparticles of approximately spherical shape and those near $n = 6$ being associated with elongated (or rod-like) nanoparticles.

When expression (9) for J_j^* and expression (11) for q_j^* are substituted into equations (3) and (4) the result is that

$$\frac{\partial \varphi^*}{\partial t^*} + V_k{}^* \frac{\partial \varphi^*}{\partial x_k{}^*} = \frac{\partial}{\partial x_k{}^*}\left(D_B \frac{\partial \varphi^*}{\partial x_k{}^*} + \frac{D_T}{T_0}\frac{\partial T^*}{\partial x_k{}^*}\right), \quad (13)$$

$$(\rho C)(\varphi^*)\left(\frac{\partial T^*}{\partial t^*} + V_k{}^* \frac{\partial T^*}{\partial x_k{}^*}\right) = \kappa(\varphi^*)\frac{\partial^2 T^*}{\partial x_k{}^* \partial x_k{}^*} + \rho_p C_p \frac{\partial T^*}{\partial x_k{}^*}\left(D_B \frac{\partial \varphi^*}{\partial x_k{}^*} + \frac{D_T}{T_0}\frac{\partial T^*}{\partial x_k{}^*}\right). \quad (14)$$

B. Boundary conditions

Thermodynamic, mechanical and nanoparticle conditions must be imposed on the boundaries $x_3{}^* = 0$ and $x_3{}^* = d$. The thermodynamic boundary conditions are embodied in the equations

$$T^*(t^*, x_\alpha{}^*, 0) = T_0, \quad (15)$$

$$q_3{}^*(t^*, x_\alpha{}^*, d) = R[T^*(t^*, x_\alpha{}^*, d) - T_1], \quad (16)$$

Where α takes the values 1 and 2, and R (constant) is the Robin parameter. The mechanical boundary conditions are embodied in the equations

$$V_k{}^*(t^*, x_\alpha{}^*, 0) = 0, \quad k = 1,2,3 \quad (17)$$

$$V_3{}^*(t^*, x_\alpha{}^*, d) = 0, \quad (18)$$

$$\sigma_{3\beta}(t^*, x_\alpha{}^*, d) = \frac{\partial \gamma}{\partial x_\beta{}^*}, \quad \beta = 1,2 \quad (19)$$

where σ_{31} and σ_{32} are the components of the surface shear stress tensor. Taking account of the condition $V_3{}^* = 0$ on $x_3{}^* = d$, the surface tension boundary conditions have simplified form

$$\frac{\partial V_\beta{}^*(t^*, x_\alpha{}^*, d)}{\partial x_3{}^*} = \frac{1}{\mu(\varphi^*)}\left[\frac{\partial \gamma}{\partial T^*}\frac{\partial T^*(t^*, x_\alpha{}^*, d)}{\partial x_\beta{}^*} + \frac{\partial \gamma}{\partial \varphi^*}\frac{\partial \varphi^*(t^*, x_\alpha{}^*, d)}{\partial x_\beta{}^*}\right]. \quad (20)$$

Finally, the most commonly used nanoparticle boundary conditions impose values for the volume fraction of nanoparticles on $x_3{}^* = 0$ and $x_3{}^* = d$. While such nanoparticle conditions provide a well-posed mathematical problem, we would argue that these conditions are unrealistic. In practice it is the total volume of nanoparticles in the nanofluid that is known. The distribution of these particles, however, depends on the prevailing temperature distribution within the nanofluid. What can be asserted with confidence is that the fluxes of nanoparticles crossing the boundaries $x_3{}^* = 0$ and $x_3{}^* = d$ are zero. Consequently, appropriate boundary conditions are

$$J_3{}^*(t^*, x_\alpha{}^*, 0) = J_3{}^*(t^*, x_\alpha{}^*, d) = 0, \quad (21)$$

subject to the constraint that

$$\lim_{|A|\to\infty} \frac{1}{|A|}\int_A \left(\frac{1}{d}\int_0^d \varphi^*(t^*, x_\alpha{}^*, x_3{}^*)\, dx_3{}^*\right) dx_\alpha{}^* = \bar{\varphi}, \quad (22)$$

where A is an arbitrary region of the $(x_1{}^*, x_2{}^*)$ plane enclosing area $|A|$.

C. Steady state solution

Equations (1), (8), (13) and (14) have a steady state solution in which the nanofluid is at rest and all other variables are functions of $x_3{}^*$ alone. The steady state solution therefore satisfies the equations

$$\frac{\partial P^*}{\partial x_3{}^*} = -\left[\varphi^* \rho_p + \rho_0 (1-\varphi^*)\left(1 - \beta(T^* - T_0)\right)\right] g,$$

$$\frac{\partial J_3{}^*}{\partial x_3{}^*} = 0, \qquad \frac{\partial q_3{}^*}{\partial x_3{}^*} = 0 \quad (23)$$

with associated boundary conditions

$$T^*(0) = T_0, \quad (24)$$

$$q_3{}^*(d) = R[T^*(d) - T_1], \quad (25)$$

$$J_3{}^*(0) = J_3{}^*(d) = 0, \quad (26)$$

subject to the constraint that

$$\frac{1}{d}\int_0^d \varphi^*(x_3{}^*)\, dx_3{}^* = \bar{\varphi}. \quad (27)$$

Let $T^* = T(x_3{}^*)$, $\varphi^* = \varphi(x_3{}^*)$ and $P^* = P(x_3{}^*)$ denote the solution of the steady state problem, then it follows from the definition of $J_j{}^*$ in expression (9) that T and φ satisfy

$$D_B \frac{d\varphi}{dx_3{}^*} + \frac{D_T}{T_0}\frac{dT}{dx_3{}^*} = 0, \quad (28)$$

in view of the second of equations (23) and the boundary conditions (26). Thus

$$D_B \varphi + D_T \frac{T}{T_0} = \text{Constant} = D_B \varphi_0 + D_T, \quad (29)$$

where φ_0 is the volume fraction of nanoparticles on the lower boundary $x_3{}^* = 0$. Equation (30) determines how changing temperature influences the distribution of nanoparticles throughout the layer of nanofluid. It follows from equation (14) that $T(x_3{}^*) = T_0 + A x_3{}^*$, where A is an arbitrary constant to be determined by the boundary condition (25), namely

$$\kappa(\varphi)\frac{dT}{dx_3{}^*} + R[T(d) - T_1] = 0. \quad (30)$$

Straightforward calculation reveals that the steady state distributions of temperature and nanoparticles are respectively

$$T(x_3{}^*) = T_0 + \frac{R(T_1 - T_0)}{\kappa(\varphi) + Rd} x_3{}^*, \quad (31)$$

$$\varphi(x_3{}^*) = \varphi_0 + \frac{D_T}{D_B}\frac{R(T_0 - T_1)}{T_0(\kappa(\varphi) + Rd)} x_3{}^*. \quad (32)$$

Finally, the value of φ_0 is determined by asserting that the average nanoparticle volume fraction across the layer is $\bar{\varphi}$, i.e. by demanding that

$$\frac{1}{d}\int_0^d \varphi(x_3{}^*)\, dx_3{}^* = \bar{\varphi}.$$

Calculation based on expression (32) yields

$$\varphi_0 = \bar{\varphi} - \frac{D_T}{D_B}\frac{R(T_0 - T_1)}{T_0(\kappa(\varphi) + Rd)}\frac{d}{2}, \quad (33)$$

$$\varphi_1 = \overline{\varphi} + \frac{D_T}{D_B}\frac{R(T_0 - T_1)}{T_0\,(\kappa(\varphi) + Rd)}\frac{d}{2}. \qquad (34)$$

The remaining of the steady state solution is obtained by substituting for T and φ in the first of equations (23) and then using integration to obtain $P(x_3^*)$.

D. Linearized and non-dimensional equations

Following standard procedures we introduce the infinitesimal perturbations $\varepsilon V_k e_k$ of fluid velocity V_k^*, εp of pressure P^*, $\varepsilon\theta$ of temperature $T(x_3^*)$, $\varepsilon\psi$ of nanoparticle volume fraction $\varphi(x_3^*)$, $\varepsilon J_k e_k$ of nanoparticle flux J_k^* and $\varepsilon q_k e_k$ of heat flux $Q_k(x_3^*)$. Thus the non-dimensional linearized form of equations (1), (8), (13) and (14) is

$$\frac{\partial V_k}{\partial x_k} = 0, \qquad (35)$$

$$\frac{1}{P_r}\frac{\rho(\overline{\varphi})}{\rho_f}\frac{\partial V_k}{\partial t} = -\frac{\partial P}{\partial x_k} + \frac{\mu(\overline{\varphi})}{\mu_f}\frac{\partial^2 V_k}{\partial x_j \partial x_j} - Rn\ \psi\ \delta_{k3} + Ra\,\theta\,\delta_{k3}, \qquad (36)$$

$$Le\left(\frac{\partial \psi}{\partial t} + H V_3\right) = \frac{\partial^2 \psi}{\partial x_k \partial x_k} + N_A \frac{\partial^2 \theta}{\partial x_k \partial x_k}, \qquad (37)$$

$$\frac{(\rho C)(\overline{\varphi})}{\rho_f C_f}\left(\frac{\partial \theta}{\partial t} - H V_3\right) = \frac{\kappa(\overline{\varphi})}{\kappa_f}\frac{\partial^2 \theta}{\partial x_k \partial x_k} - H\frac{N_B}{Le}\left(\frac{\partial \psi}{\partial x_3} + N_A \frac{\partial \theta}{\partial x_3}\right). \qquad (38)$$

where $H = sign(T_0 - T_1)$ and the concentration Rayleigh number Rn, the thermal Rayleigh number Ra, the Lewis number Le, the Prandtl number P_r, the modified diffusivity ratio N_A and the modified particle density increment N_B are defined by the respective expressions

$$Rn = \frac{(\rho_p - \rho_f)|\varphi_1 - \varphi_0|\,g\,d^3}{\alpha\,\mu_f}, \qquad Ra = \frac{\rho_f\,g\,\beta\,d^3\,|T(d) - T_0|}{\alpha\,\mu_f},$$

$$Le = \frac{\alpha}{D_B}, \qquad P_r = \frac{\mu_f\,C_f}{\kappa_f}, \qquad N_A = \frac{D_T\,|T(d) - T_0|}{D_B\,T_0\,|\varphi_1 - \varphi_0|},$$

$$N_B = \frac{\rho_s\,C_s}{\rho_f\,C_f}|\varphi_1 - \varphi_0|.$$

The values of φ_0, φ_1 and $T(d)$ are determined directly from the stationary solution. Equations (35- 38) give the general form of the non-dimensional linearized equations.

The non-dimensional linearized boundary conditions on the lower boundary $x_3^* = 0$ require that

$$V_3 = 0, \qquad (39)$$

$$\frac{\partial V_3}{\partial x_3} = 0, \qquad (40)$$

$$\theta = 0, \qquad (41)$$

$$\frac{\partial \psi}{\partial x_3} + N_A \frac{\partial \theta}{\partial x_3} = 0, \qquad (42)$$

The non-dimensional linearized boundary conditions on the upper boundary $x_3^* = 1$ require that

$$V_3 = 0, \qquad (43)$$

$$\frac{\partial^2 V_3}{\partial x_3^{\,2}} = M_T \Delta_2 \theta + M_\varphi \Delta_2 \psi, \qquad (44)$$

$$\frac{\kappa(\overline{\varphi})}{\kappa_f}\frac{\partial \theta}{\partial x_3} + Nu\,\theta = 0, \qquad (45)$$

$$\frac{\partial \psi}{\partial x_3} + N_A \frac{\partial \theta}{\partial x_3} = 0, \qquad (46)$$

In these conditions M_T is the temperature Marangoni number, M_φ is the nanoparticle Marangoni number and Nu is the Nusselt number with respective definitions

$$M_T = -\frac{\partial \gamma}{\partial T}\frac{d\,|T(d) - T_0|}{\alpha\,\mu(\overline{\varphi})}, \qquad M_\varphi = -\frac{\partial \gamma}{\partial \varphi}\frac{d\,|\varphi_1 - \varphi_0|}{\alpha\,\mu(\overline{\varphi})},$$

$$Nu = \frac{R\,d}{\kappa_f}$$

III. NORMAL MODE ANALYSIS

A normal mode analysis is used in which

$$(V_3,\ \theta, \psi) = (w(x_3), \theta(x_3), \psi(x_3))\,e^{\sigma t + in\,x_1 + im\,x_2} \qquad (47)$$

where n, m are the wave numbers along the e_1 and e_2 directions respectively and σ is a growth rate. The eigenvalue problem for σ is constructed by the conventional procedure and becomes

$$\frac{\sigma}{P_r}\frac{\rho(\overline{\varphi})}{\rho_f} Lw = \frac{\mu(\overline{\varphi})}{\mu_f} L^2 w, \qquad (48)$$

$$Le\,(\sigma\,\psi + H\,w) = L\psi + N_A\,L\theta, \qquad (49)$$

$$\frac{(\rho C)(\overline{\varphi})}{(\rho\,C)_f}(o\,\theta - H\,w) = \frac{\kappa(\overline{\varphi})}{\kappa_f}\,L\theta - H\,\frac{N_B}{Le}\left(\frac{d\psi}{dx_3} + N_A\frac{d\theta}{dx_3}\right). \qquad (50)$$

where $L(g) = \frac{d^2 g}{dx_3^{\,2}} - a^2\,g,$ and $a = \sqrt{n^2 + m^2}$.

Equations (48 - 50) are solved with conditions

$$w(1) = \frac{d^2 w(1)}{dx_3^{\,2}} + a^2 M_T \theta(1) + a^2 M_\varphi \psi(1) = 0, \qquad (51)$$

$$\frac{\kappa(\overline{\varphi})}{\kappa_f}\frac{d\theta(1)}{dx_3} + Nu\,\theta(1) = \frac{d\psi(1)}{\partial x_3} + N_A\frac{d\theta(1)}{dx_3} = 0, \qquad (52)$$

on the upper surface and base conditions

$$w(0) = \frac{dw(0)}{dx_3} = 0, \qquad (53)$$

$$\theta(0) = \frac{d\psi(0)}{dx_3} + N_A\frac{d\theta(0)}{dx_3} = 0. \qquad (54)$$

IV. R ESULTS AND DISCUSSION

Given values for N_A, N_B, Le, Nu, Rn and P_r and constitutive expressions for $\rho(\overline{\varphi}), \mu(\overline{\varphi}), (\rho C)(\overline{\varphi})$ and $\kappa(\overline{\varphi})$ the task is to determine the critical boundary for the Rayleigh number, Ra, and the Marangoni numbers, M_T and M_φ, separating stable combinations from unstable combinations.

Fig. 1 illustrates the stability boundaries for the Rayleigh and temperature Marangoni numbers in the case of an ethanol-alumina nanofluid with a 0.2% volume fraction of nanoparticles when $M_\varphi = 10$

(dashed line), $M_\varphi = 30$ (solid line) and $M_\varphi = 100$ (dotted line) when the heat transfer coefficient (Robin constant) has values $R = 10$ (Fig. 1a) and $R = 100$ R = 100 (Fig. 1b).

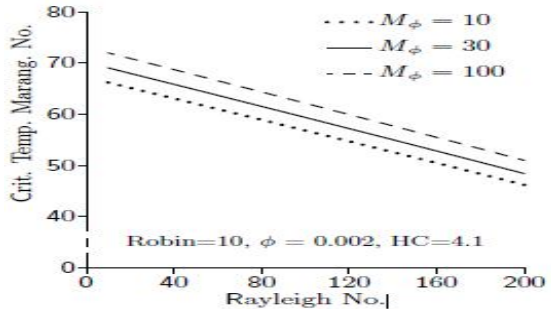


Fig. 1a: The critical stability boundaries for the Rayleigh and temperature Marangoninumbers are illustrated for an ethanol-alumina nanofluid with a 0.2% volume nano-fraction when $M_\varphi = 10$ (dashed line), $M_\varphi = 30$ (solid line) and $M_\varphi = 100$ (dotted line) for R = 10.

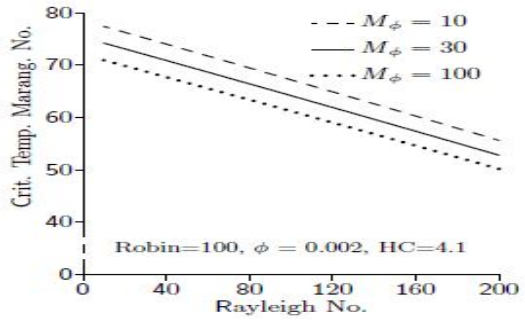


Fig. 1b: The critical stability boundaries for the Rayleigh and temperature Marangoni numbers are illustrated for an ethanol-alumina nanofluid with a 0.2% volume nano-fraction when $M_\varphi = 10$ (dashed line), $M_\varphi = 30$ (solid line) and $M_\varphi = 100$ (dotted line) for R = 100.

Fig. 2 illustrates the equivalent stability boundaries for the Rayleigh and temperature Marangoni numbers for an ethanol-alumina nanofluid with a 1% volume fraction of nanoparticles when $M_\varphi = 10$ (dashed line), $M_\varphi = 30$ (solid line) and $M_\varphi = 100$ (dotted line) when the heat transfer coefficient (Robin constant) has values $R = 10$ (Fig. 2a) and $R = 100$ R = 100 (Fig. 2b).

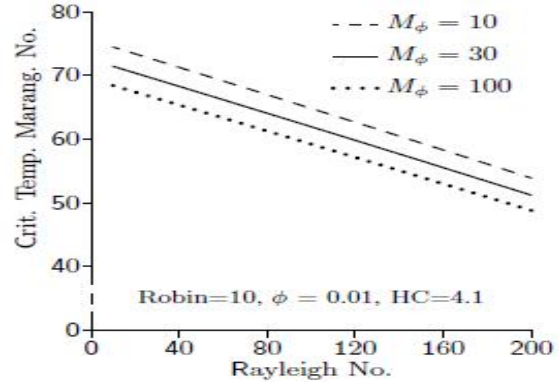


Fig. 2a: The critical stability boundaries for the Rayleigh and temperature Marangoni numbers are illustrated for an ethanol-alumina nanofluid with a 1% volume nano-fraction when $M_\varphi = 10$ (dashed line), $M_\varphi = 30$ (solid line) and $M_\varphi = 100$ (dotted line) for R = 10.

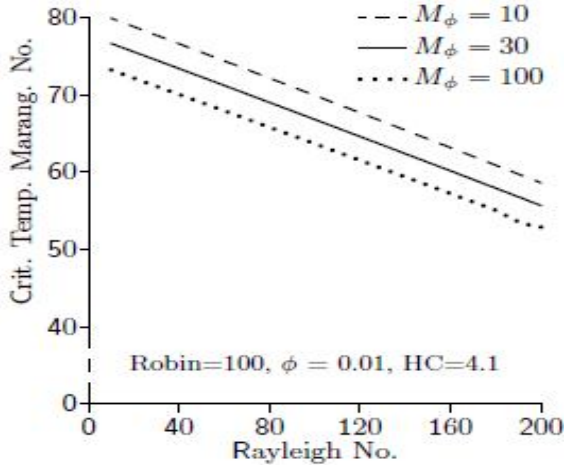


Fig. 2b: The critical stability boundaries for the Rayleigh and temperature Marangoni numbers are illustrated for an ethanol-alumina nanofluid with a 1% volume nano-fraction when $M_\varphi = 10$ (dashed line), $M_\varphi = 30$ (solid line) and $M_\varphi = 100$ (dotted line) for R = 100.

The literature reveals that the mode of instability in Rayleigh-Marangoni convection for non-deformable surfaces is always of a stationary type. In this problem instability always occurs via an overstable mode. Although not reported here in detail, ethanol-MWCNTs nanofluids exhibit similar behavior to that illustrated in Figs. 1 and 2. The critical (Ra, M_T) boundary curve for these nanofluids lie above the comparable curves for the ethanol-alumina nanofluids. Thus an ethanol-Alumina nanofluid is less stable than that of the equivalent ethanol-MWCNTs nanouid with identical values of Ra and M_φ.

Figs. 1 and 2 illustrate the following behaviours.

1. The stability boundary is relatively insensitive to the nature of the nanoparticle in this application, although a detailed inspection reveals that the ethanol-alumina nanofluid is marginally less stable than the ethanol-MWCNT nanofluid.
2. Critical values of M_T decrease for positive increasing values of M_φ indicating that M_φ has a destabilizing effect on the system.
3. Calculations reveals that heating this configuration of nanofluid from below and cooling the top surface by convection is always unstable whenever M_φ takes negative values.
4. Figs. 1 and 2 illustrate that the critical values of M_T increase as φ increases. Thus increasing the average volume fraction of nanoparticles in an ethanol-alumina or ethanol-MWCNT nanofluid has a stabilizing influence for fixed positive values of Ra and M_φ.
5. Similarly, it is clear from Figs. 1 and 2 that increasing the value of the surface heat transfer coefficient, R, improves the stability of the ethanol-alumina and ethanol-MWCNT nanofluids.

ACKNOWLEDGMENT

The authors are grateful for the financial support for this project from King Abdulaziz City of Science and Technology, Saudi Arabia through its National Science, Technology and Innovation Plan (Research project No. 12-MAT2314-10).

REFERENCES

[1] J. Buongiorno, and L. Hu, “Nanofluid coolants for advanced nuclear power plants,” Proceedings of ICAPP '05, Seoul, Paper no. 5705. 2005.
[2] T. Tsai, and R. Chein, "Performance analysis of nanofluid-cooled microchannel heat sinks," Int. J. Heat Fluid Flow, vol. 28, pp 1013-1026, 2007.
[3] C. Kleinstreuer, J. Li, and J. Koo, "Microfluidics of nano-drug delivery," Int. J. Heat Mass Trans., vol. 51, pp 5590-5597, 2008.
[4] J. Buongiorno, "Convective transport in nanofluids," J. Heat Trans. ASME, vol. 128, pp 240-250, 2006.
[5] D. Tzou, "Thermal instability of nanofluids in natural convection," Int. J. Heat Mass Trans., vol. 51, pp 2967-2979, 2008.
[6] D. Tzou, "Instability of nanofluids in natural convection," J. Heat Trans. ASME, vol. 130. no. 7, pp 072401, 2008.
[7] D. Nield and A. Kuznetsov, "Thermal instability in a porous medium layer saturated by a nanofluid," Int. J. Heat Mass Trans., vol. 52, pp 5796-5801, 2009.
[8] D. Nield and A. Kuznetsov, "The onset of convection in a horizontal nanofluid layer of finite depth," Euro. J. Mech. B/Fluids, vol. 29, pp 217-223, 2010.
[9] A. Kuznetsov and D. Nield, "The onset of double diffusive nanofluid convection in a layer of a saturated porous medium," Trans. Porous Media, vol. 85, pp 941-951, 2010.
[10] A. Kuznetsov and D. Nield, " Effect of local thermal non-equilibrium on the onset of convection in a porous medium layer saturated by a nanofluid," Trans. Porous Media, vol. 83, pp 425-436, 2010.
[11] A. Kuznetsov and D. Nield, " Effect of local thermal non-equilibrium on the onset of convection in a porous medium layer saturated by a nanofluid," Trans. Porous Media, vol. 83, pp 425-436, 2010.
[12] D. Yadav, G. Agrawal and R. Bhargava, "Thermal instability of rotating nanofluid layer," Int. J. Eng. Sci., vol. 49, pp 1171-1184, 2011.
[13] C. Ramesh and G. Rana, "On the onset of thermal convection in rotating nanofluid layer saturating a Darcy-Brinkman porous medium," Int. J. Heat Mass Trans., vol. 55, pp 5417-5424, 2012.
[14] U. Gupta, J. Ahuja and R. Wanchoo, "Magneto convection in a nanofluid layer," Int. J.Heat Mass Trans., vol. 64, pp 1163-1171, 2013.
[15] D. Yadav, R. Bhargava and G. Agrawal, "Thermal instability in a nanofluid layer with a vertical magnetic field," J. Eng. Math., vol. 80, pp 147-164, 2013.
[16] A. Mahajan and M. Arora, "Convection in rotating magnetic nanofluids," Appl. Math. Comp., vol. 219, pp 6284-6296, 2013.
[17] A. Abdullh and K. Lindsay, "Marangoni convection in a thin layer of nanofluid: Application to combinations of water or ethanol with nanoparticles of alumina or multi-walled carbon nanotubules," Int. J. Heat Mass Trans., To be published.
[18] D. Nield, "Surface tension and buoyancy effects in cellular convection," J. Fluid Mech., vol. 19, pp 341-352, 1964.
[19] G. Sarma, "Benard-Marangoni instability in a rotating liquid layer subjected to a transverse magnetic field," Adv. Space Res., vol. 3, no. 5, pp 33-36, 1983.
[20] P. Garcia-Ybarra, J. Castillo and G. Velarde, "Benard-Marangoni convection with a deformable interface and poorly conducting boundaries," Phys. Fluids, vol. 30, no. 9, pp 2655-2661, 1987.
[21] R. Benguria and M. Depassier, "On the linear stability theory of Benard-Marangoni convection," Phys. Fluids A, vol. 1, no. 7, pp 1123-1127, 1989.
[22] C. Perez-Garcia and G. Carneiro, "Linear stability analysis of Benard-Marangoni convection in fluids with a deformable free surface," Phys. Fluids, vol. 3, no. 2, pp 292-298, 1991.
[23] M. Hennenberg, M. Saghir, A. Rednikov and J. Legros, "Porous media and the Benard-Marangoni problem," Trans. Porous Media, vol. 27, pp 327-355, 1997.
[24] I. Hashim and N. Arfin, "Oscillatory Marangoni convection in a conducting fluid layer with a deformable free surface in the presence of a vertical magnetic field," Acta Mech. Vol. 164, pp 199-215, 2003.
[25] H.C. Brinkman, "The viscosity of concentrated suspensions and solutions," J. Chem. Phys., vol. 20, pp 571-581, 1952.
[26] R. Hamilton and O. Crosser, "Thermal conductivity of heterogeneous two-component systems," Indus. Eng. Chem. Fund., vol. 1, no. 3, pp 187-191, 1962.
[27] E.V. Timofeeva, J.L. Routbort and D. Singh,"Particle shape effects on thermophysical properties of alumina nanofluids," J. Appl. Phys., vol. 106, 2009, 014304-1, 014304-6.

★★★